Catalysis Today 143 (2009) 9–16

Contents lists available at ScienceDirect

Catalysis Today

journal homepage: www.elsevier.com/locate/cattod

Reforming of methane over noble metal catalysts: Catalyst deactivation induced by thiophene

J. Requies [a,*], S. Rabe [b], F. Vogel [b], T.-B. Truong [b], K. Filonova [b], V.L. Barrio [a], J.F. Cambra [a], M.B. Güemez [a], P.L. Arias [a]

[a] School of Engineering (UPV/EHU), c/Alameda Urquijo s/n, 48013 Bilbao, Spain
[b] Paul Scherrer Institut, Laboratory for Energy and Materials Cycles, 5232 Villigen PSI, Switzerland

ARTICLE INFO

Article history:
Available online 11 December 2008

Keywords:
Ruthenium
Rhodium
Sol–gel
Thiophene
Methane
LTCPO
Sulphur

ABSTRACT

This work is focused on the performance of rhodium and ruthenium catalysts for the low temperature wet catalytic partial oxidation (LTCPO) of methane in sulphur-free conditions and also at different sulphur concentrations. Catalysts characterization was conducted by X-ray diffraction (XRD), BET surface area measurements, X-ray photoelectron spectroscopy (XPS), O_2 chemisorption by TGA, and transmission electron microscopy (TEM). All of the catalysts showed a high activity and selectivity towards hydrogen if sulphur-free reaction conditions were applied. The presence of small amounts of thiophene (10 ppm) in the feed decreased the activity for all the catalysts. However, at this concentration one ruthenium catalyst showed a high sulphur tolerance. For all the rhodium catalysts a strong deactivation and a higher CO_2 selectivity was observed at 10 ppm of thiophene. Operation with 400 ppm of thiophene in the feed resulted in a low activity for both Rh and Ru catalysts, and only a small amount of CO_2 was produced.

1. Introduction

The reforming process for hydrogen/syngas generation via steam reforming (SR), catalytic partial oxidation (CPO), or autothermal reforming (ATR) are the main commercially competitive methods to hydrogen production from petroleum-based fuels [1]. Nowadays, syngas is mainly produced from natural gas by the steam reforming of methane (SRM). An alternative process, the low temperature catalytic partial oxidation (LTCPO), a combination of endothermic SRM and exothermic CPO [2], is carried out at lower temperatures than SRM and CPO (Eq. (1)). Due to the lower process temperature the cost of hydrogen is expected to be lower, because cheaper materials of construction could be used, reducing the investment and operating cost [2]:

$$CH_4 + 0.5O_2 + H_2O \rightarrow CO_2 + 3H_2 \quad (1)$$

The composition of natural gas varies in time as well as in provenance, with respect to hydrocarbons concentrations and sulphur impurities. The sulphur compounds typically present in natural gas are hydrogen sulphide (H_2S), carbon oxysulphide (COS), and organic sulphides (R–S–R′), disulphides (R–S–S–R′), mercaptans (R–SH), and carbon disulphide (CS_2). For reasons of transportation safety it is necessary to remove the sulphur compounds. Nevertheless after this treatment, natural gas still contains trace amounts of H_2S, COS, CS_2, and short chain R–SH and R–S–R′ [3]. In addition, for safety an odorant is added before natural gas distribution. For USA, UK and Japan this sulphur odorant used to be based on mercaptan mixtures, while in most of Europe tetrahydrothiophene (THT) is preferred [3]. Typical odorant concentrations are 15–20 mg/m^3 for THT and 5–7 mg/m^3 for mercaptan mixtures, but short duration peaks in sulphur content up to 150 mg/m^3 are allowed [3]. These small amounts of sulphur compounds are able to deactivate the catalytic system by their poisonous effect; hence the sulphur compounds have to be removed from the feed prior to hydrogen production [4]. An attractive possibility to avoid or reduce the effort for desulphurization is to develop sulphur resistant catalysts.

In the industrial production of H_2 the most widely used catalysts consist of nickel supported on modified alumina or mixed metal oxides, although the noble metals Pd, Rh, and Ru are active as well for these processes [5]. Nickel is preferred due to its lower cost [5,6]. Nevertheless, noble metals have gained increasing interest

* Corresponding author at: School of Engineering (UPV/EHU), Chemical and Environmental Engineering, c/Alameda Urquijo s/n, 48013 Bilbao, Spain. Tel.: +34 946017482; fax: +34 946014179.
E-mail address: jesus.requies@ehu.es (J. Requies).

0920-5861/$ – see front matter © 2008 Elsevier B.V. All rights reserved.
doi:10.1016/j.cattod.2008.10.026

Table 1
Summary of the preparation of the catalysts.

Catalyst	Calcination temperature	Remark (method)	Support (manufacturer)	Ru (wt%)	Rh (wt%)
$5Ru/Al_2O_3$ 550 w.i.	550 °C (3 h) in air		γ-Al_2O_3 (Johnson Matthey)	5	
$5Ru/Al_2O_3$ 800 w.i.	800 °C (3 h) in air		γ-Al_2O_3 (Johnson Matthey)	5	
$5Ru/Al_2O_3$ s.g. 1	550 °C in N_2/H_2 mixture	Without water distillation before the preparation	γ-Al_2O_3 (Johnson Matthey)	5	
$5Ru/Al_2O_3$ s.g. 2	550 °C in N_2/H_2 mixture	Water was distilled from the Ru solution before preparation	γ-Al_2O_3 (UOP)	5	
$5Ru/Al_2O_3$ s.g. 3	550 °C in N_2/H_2 mixture	Water was distilled from the Ru solution before preparation	γ-Al_2O_3 (UOP)	5	
$1Rh/5Ce–ZrO_2$ w.i.	550 (3 h)		ZrO_2 (DKKK)		1
$1Rh/5Ce–ZrO_2$ s.g.	550 °C in N_2/H_2 mixture		ZrO_2 (DKKK)		1

for hydrogen production due to their highest intrinsic rates for hydrogen production and strongly reduced coke formation [5,7,8]. Many studies have been published on the production of hydrogen in the presence of noble metals, but only few studies have been done in the presence of sulphur compounds. No studies have been published on LTCPO in the presence of thiophene. The purpose of this work was to investigate the effect of catalyst preparation, and different thiophene concentrations in the feed, on the sulphur tolerance of rhodium and ruthenium catalysts for the LTCPO of methane.

2. Experimental

2.1. Catalyst preparation

Ruthenium and rhodium catalysts were prepared by two methods: sol–gel (s.g.) and wetness impregnation (w.i.). For wetness impregnation, aqueous rhodium and ruthenium nitrate solutions were used. Support materials used were ceria doped-zirconium dioxide (DKKK, Japan), and γ-alumina (Johnson Matthey (JM) and UOP). After impregnation and drying, the sample was calcined in air at 550 °C for 3 h, and in the case of the ruthenium also up to 800 °C. The sol–gel preparation procedures were different for the ruthenium and rhodium catalysts. The Ru/Al_2O_3 catalysts were prepared by reduction of a $RuCl_3$ solution with ethylene glycol in the presence of γ-alumina (JM and UOP) and sodium acetate (CH_3COONa) to prevent particle growth. The ruthenium solution was added under stirring to the ethylene glycol and CH_3COONa. Then, the alumina was added to form a suspension. After this, the suspension was slowly heated to 180 °C while stirring and kept at this temperature for 10 min (about 15 min for $5Ru/Al_2O_3$ s.g. 3). To reach this temperature it is necessary to remove the water. For Ru/Al_2O_3 s.g. 2 and 3, the water was removed by distillation *before* heating up, while for Ru/Al_2O_3 s.g. 1, the water was removed by distillation during the heating up. The time it takes to reduce the catalyst (at 180 °C) has a big influence on the particle size. Particles may become bigger with increasing reduction time, while at short reduction times the ruthenium is not completely reduced [9]. After the reduction the catalyst was filtered with the addition of sodium nitrate, dried and calcined in the reactor system with an N_2/H_2 (3:1, v/v) mixture at 550 °C. The sol–gel preparation of the rhodium catalysts was more complex. The catalysts were prepared similar to the procedure reported by Schulz et al. [10] and De Rogatis et al. [11]. An aqueous solution of $NaBH_4$ and *N*-hexadecyl-*N*-(2-hydroxyethyl)-*N*,*N*-dimethyl ammonium bromide was added under vigorous stirring to an aqueous solution of $Rh(NO_3)_3$ at room temperature. After 2 h the modified support $5Ce–ZrO_2$ was added. The resulting suspension was added dropwise to a 10% NH_4OH solution under vigorous stirring. After 1 h the suspension was filtered and washed to eliminate the bromide. After the second filtration the catalyst was dried at 393 K overnight. The catalyst was also calcined at 550 °C in the reactor system with an N_2/H_2 (3:1, v/v) mixture. All the catalysts are summarized in Table 1. The fresh and spent catalysts were characterized by X-ray diffraction (XRD; Philips diffractometer using FeKα radiation at 1.9360 nm), and X-ray photoelectron spectroscopy (XPS). The fresh catalysts were also characterized by BET surface measurements, transmission electron microscopy (TEM), and the active metal dispersion was determined by O_2 chemisorption using TGA. This technique is based on a reduction at 300 °C followed by an oxidation at room temperature. The dispersion was calculated as $n_{Ru,s}/n_{Ru}$ (atomic ruthenium at the surface to total nominal ruthenium).

2.2. Activity measurements

The experiments were conducted in a fixed-bed microreactor. The microreactor (glass lined stainless steel tube, 4 mm inner diameter) was heated electrically in a furnace. The effluent stream was cooled down, condensed water was collected and weighed, and the gas phase was analyzed online by a GC (Agilent 6890) equipped with FID and TCD detectors. The activity measurements were carried out at atmospheric pressure at an oven setpoint of 550 °C with a feed of $CH_4/O_2/N_2 = 2/1/3.8$ (molar ratio), and at a WHSV of 65 $g_{feed}\ g_{cat}^{-1}\ h^{-1}$. In all the experiments the total flow was 62.2 mL/min at normal conditions. A steam to carbon ratio (S/C) of 2 was applied. The particle size range was 125–250 μm. The catalyst (sample weight 100 mg) was diluted with SiC at a ratio of 1:4.5 to minimize the hot spot in the bed (bed length approximately 50 mm). A thermowell (stainless steel, outer diameter 1.5 mm), equipped with a movable thermocouple, was placed in the centre of the catalyst bed in order to monitor the temperature profile along the reactor. Prior to the tests the catalysts were reduced at 550 °C and atmospheric pressure in a H_2/N_2 (1:3, v/v) mixture. Three different activity tests of 50 h each were carried out: feed free of thiophene, with 10 ppm of thiophene, and with 400 ppm of thiophene. The conversion, yields, and selectivities were calculated, based on the molar flow rates, as

$$X_{CH_4} = \frac{CH_{4,in} - CH_{4,out}}{CH_{4,in}}, \qquad X_{H_2O} = \frac{H_2O_{in} - H_2O_{out}}{H_2O_{in}},$$

$$X_{O_2} = \frac{O_{2,in} - O_{2,out}}{O_{2,in}}$$

$$Y_{CO} = \frac{CO_{out}}{CH_{4,in}}, \qquad Y_{CO_2} = \frac{CO_{2,out}}{CH_{4,in}}, \qquad Y_{H_2} = \frac{H_{2,out}}{3CH_{4,in}}$$

$$S_{CO_2} = \frac{CO_{2,out}}{CO_{2,out} + CO_{out}}$$

Table 2
Dispersion and BET surface area. A_s: metal surface area.

Catalyst	Dispersion	A_s (m^2/g_{cat})	BET (m^2/g)
$5Ru/Al_2O_3$ 550 w.i.	0.1	2.8	134
$5Ru/Al_2O_3$ 800 w.i.	0.22	5.9	103
$5Ru/Al_2O_3$ s.g. 1	0.95	25.1	131
$5Ru/Al_2O_3$ s.g. 2	0.99	26.3	231
$5Ru/Al_2O_3$ s.g. 3	0.44	11.7	234
γ-Al_2O_3 (Johnson Matthey)	–	–	124
γ-Al_2O_3 (UOP)	–	–	226
$1Rh/5Ce–ZrO_2$ w.i.	0.43	2.3	32
$1Rh/5Ce–ZrO_2$ s.g.	0.96	5.1	78
$5Ce–ZrO_2$	–	–	30

3. Results

3.1. Catalyst characterization

The ruthenium catalysts supported on alumina revealed different surface areas (103 to 234 m^2/g) according to the alumina employed (Table 2). No significant difference was observed between the two different techniques of preparation for the ruthenium catalysts. For the rhodium catalysts a lower BET surface area was observed (32 and 78 m^2/g). For the rhodium catalysts a clear influence of the preparation method (sol–gel versus impregnation) can be seen. For $1Rh/5Ce–ZrO_2$ s.g. the BET surface area was more than twice the one of $1Rh/5Ce–ZrO_2$ w.i. with the same support (30.0 m^2/g). This may be due to the formation of rhodium nanoparticles by the sol–gel method which exhibit a large metal surface area. This high dispersion was confirmed by O_2 chemisorption measurements (Table 2), and XPS. The catalysts prepared by sol–gel had a higher dispersion, and therefore the active metal surface area per gram of catalyst was also higher (A_s in Table 2). A high dispersion was also obtained for the ruthenium sol–gel catalysts. All of them had a higher dispersion and specific active metal surface area than the ones prepared by wetness impregnation. XRD patterns of the fresh rhodium and ruthenium catalysts are shown in Fig. 1. For the rhodium catalysts only reflections from the support were observed. The absence of any reflections from rhodium indicates that rhodium was dispersed on the support as very small particles for both sol–gel and wetness impregnation. The reflections observed for the rhodium catalysts corresponded to that of ZrO_2, and not to mixed Zr–Ce oxides. For ruthenium sol–gel catalysts the same behaviour was observed. No reflection from ruthenium was observed, except for the $5Ru/Al_2O_3$ 550 w.i. and $5Ru/Al_2O_3$ 800 w.i. The absence of ruthenium reflections is an indicator of a good metal dispersion. This is confirmed by the TEM picture (Fig. 2). The $5Ru/Al_2O_3$ s.g. 2 has small ruthenium particles (between 2 and 5.5 nm), and these ruthenium nanoparticles can be related to the high metal dispersion. XRD patterns of both fresh ruthenium catalysts prepared by wetness impregnation present ruthenium dioxide peaks. The crystallite size was estimated by the Scherrer formula, and for these wetness impregnation ruthenium catalysts the diameter of the metal particles was slightly bigger at the higher calcination temperature (Table 3). The XRD patterns of the used catalysts for sulphur-free conditions are presented in Figs. 3 and 4. No rhodium peak was observed. In contrast, all ruthenium catalysts (sol–gel and wetness impregnation) show metallic ruthenium peaks. These peaks were smaller for the ruthenium sol–gel catalysts than for the wetness impregnation catalysts (Table 3). The presence of ruthenium metal was recently shown for a similar catalyst using in situ XAS [12].

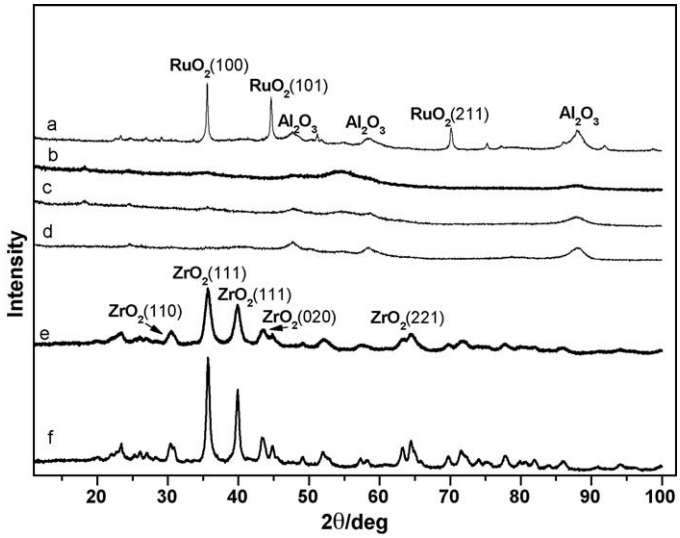

Fig. 1. XRD patterns of fresh rhodium catalysts (e and f) and ruthenium catalysts (a–d): (a) $5Ru/\gamma$-Al_2O_3 550 w.i., (b) $5Ru/\gamma$-Al_2O_3 s.g. 3, (c) $5Ru/\gamma$-Al_2O_3 s.g. 2, (d) $5Ru/\gamma$-Al_2O_3 s.g. 1, (e) $1Rh/5Ce–ZrO_2$ s.g., and (f) $1Rh/5Ce–ZrO_2$ w.i.

The binding energies of Ce $3d_{5/2}$, O 1s, Rh 3d, and Zr 3d are summarized in Table 4. Photoelectron spectra of Rh 3d levels are displayed in Fig. 5. For the fresh $1Rh/5Ce–ZrO_2$ w.i. catalyst, Rh^{3+}

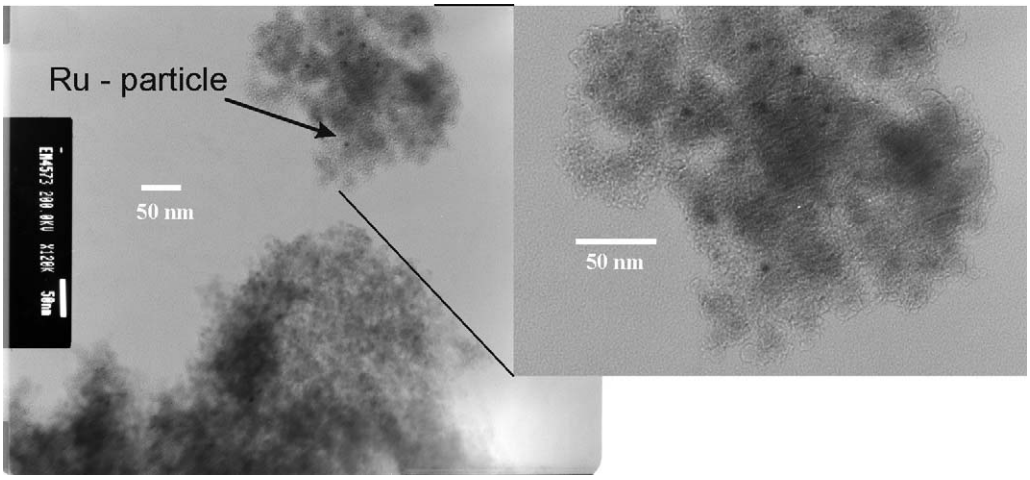

Fig. 2. TEM results of the catalyst $5Ru/\gamma$-Al_2O_3 s.g. 2 (fresh sample).

Table 3
Crystallite size estimated by the Scherrer formula for sulphur-free conditions.

Catalyst	Particle diameter (fresh)	Particle diameter (used)
5Ru/Al_2O_3 550 w.i.	37	49
5Ru/Al_2O_3 800 w.i.	42	44
5Ru/Al_2O_3 s.g. 1	n.d.	35
5Ru/Al_2O_3 s.g. 2	n.d.	29
5Ru/Al_2O_3 s.g. 3	n.d.	37
1Rh/5Ce–ZrO_2 w.i.	n.d.	n.d.
1Rh/5Ce–ZrO_2 s.g.	n.d.	n.d.

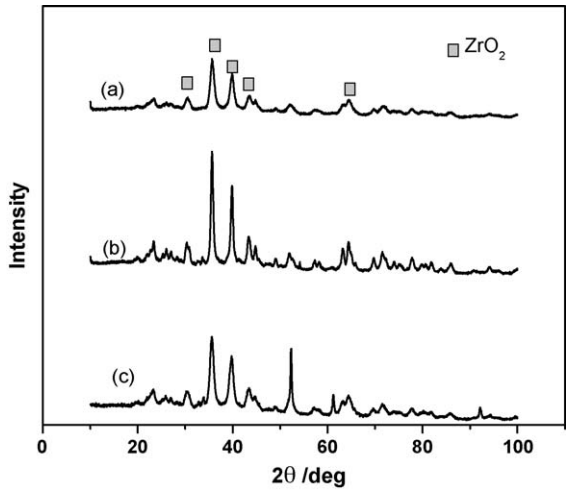

Fig. 3. XRD patterns of the rhodium catalysts for fresh w.i. catalysts (a), and used catalysts in sulphur-free conditions (b and c): (a) 1Rh/5Ce–ZrO_2 w.i., (b) 1Rh/5Ce–ZrO_2 w.i., and (c) 1Rh/5Ce–ZrO_2 s.g.

was the only species detected, as deduced from the binding energy at 308.6 eV [13,14]. In the case of the fresh 1Rh/5Ce–ZrO_2 s.g. the only detected species was Rh^0 (binding energy at 307 eV) [13,14]. In the case of Ce $3d_{5/2}$, Zr 3d, and O 1s no difference was observed between the two catalysts. For Ce $3d_{5/2}$ the presence of the Ce^{4+} species was confirmed (at 882.2–882.7 eV) [13], and the Zr 3d peak at 181.7–182.1 eV corresponds to ZrO_2. Table 4 also summarizes the surface composition derived from the XPS analysis. It was also

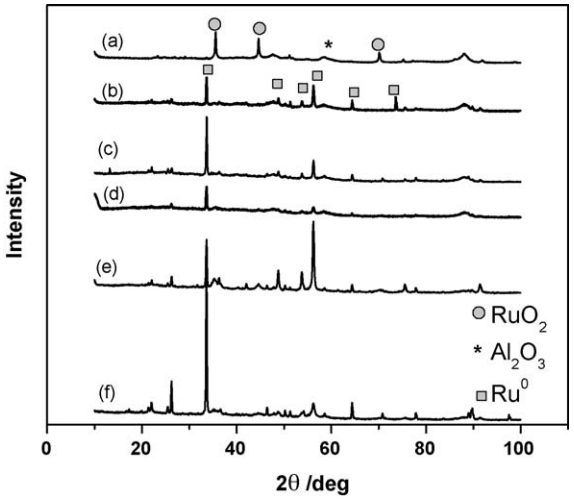

Fig. 4. XRD patterns of the ruthenium catalysts for fresh w.i. catalysts (a) and used catalysts in sulphur-free conditions (b–f): (a) 5Ru/γ-Al_2O_3 550, (b) 5Ru/γ-Al_2O_3 550 (c) 5Ru/γ-Al_2O_3 800, (d) 5Ru/γ-Al_2O_3 s.g. 1, (e) 5Ru/γ-Al_2O_3 s.g. 2, and (f) 5Ru/γ-Al_2O_3 s.g. 3.

Table 4
Binding energies (eV) of catalyst core-levels, and Rh/Zr surface atomic ratio.

Catalyst	Ce $3d_{5/2}$	O 1s	Rh 3d	Zr 3d	Rh/Zr ratio
1Rh/5Ce–ZrO_2 w.i. (fresh)	882.2	529.7	308.6	181.7	0.025
1Rh/5Ce–ZrO_2 w.i. (sulphur)	883.0	530.0	308.5	181.9	0.023
1Rh/5Ce–ZrO_2 s.g. (fresh)	882.7	528.7	307.0	181.8	0.13
1Rh/5Ce–ZrO_2 s.g. (sulphur)	884.8	530.2	308.7	182.1	0.13

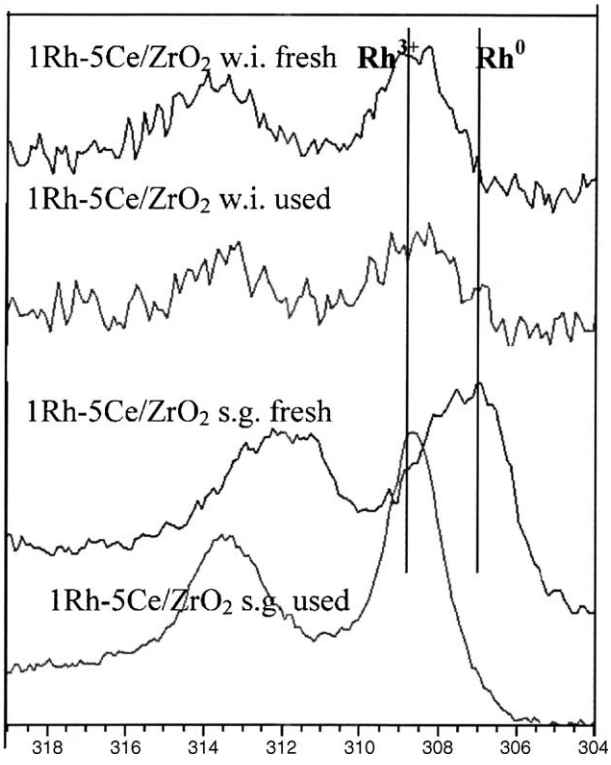

Fig. 5. X-ray photoelectron spectra of the Rh 3d for fresh and used catalysts.

observed that the catalysts prepared by sol–gel had more active metal at the surface than the wetness impregnation ones, confirming the previous dispersion data. After using these rhodium catalysts in the LTCPO of methane in the presence of 400 ppm of thiophene, no sulphur compounds (S 2p) were observed. The Rh species present in the two catalysts was Rh_2O_3 (at 308.5–308.7 eV) [13,14], nevertheless the dispersion was maintained in the two catalysts. The oxidation state of ZrO_2 did not change but the peak of Ce 3d was shifted to a value of 883–884.8 eV during the reaction. Hence, the Ce-ion was reduced under LTCPO conditions, documented by the presence of Ce^{3+} species. For the ruthenium catalysts the following orbitals were measured: Ru 3p, O 1s, Al 2p and 2 S. The amount of ruthenium on the surface was very low. Therefore, the oxidation state of ruthenium could not be determined. Nevertheless it seems that the dispersion is higher for the fresh sol–gel catalysts (Table 5). The Ru/Al ratio of the fresh catalysts is higher than for the used catalysts which may indicate a loss of dispersion by sintering effects. Another possibility could be a loss of ruthenium which was observed during the autothermal reforming over a structured Ru/Al_2O_3 catalyst [15]. When thiophene was present in the feed at 400 ppm, the dispersion was decreased, and the presence of sulphur on the catalytic surface was detected for 5Ru/Al_2O_3 s.g. 1 after the reaction. As shown in Table 5 these catalysts presented a peak assigned to SO_4^{2-} at

Table 5
Binding energies (eV) of catalyst core-levels, and Ru/Al surface atomic ratio.

Catalyst	Ru 3p	O 1s	S 2p	Al 2p	Ru/Al ratio
5Ru/Al_2O_3 w.i. 550 (fresh)	460.8	46.7	–	74.4	0.0051
5Ru/Al_2O_3 w.i. 550 (used)	461.9	47.7	–	74.4	0.0042
5Ru/Al_2O_3 s.g. 1 (fresh)	460.6	45.7	n.d.	74.4	0.01
5Ru/Al_2O_3 s.g. 1 (used)	463.0	52.2	169.1	74.4	0.006

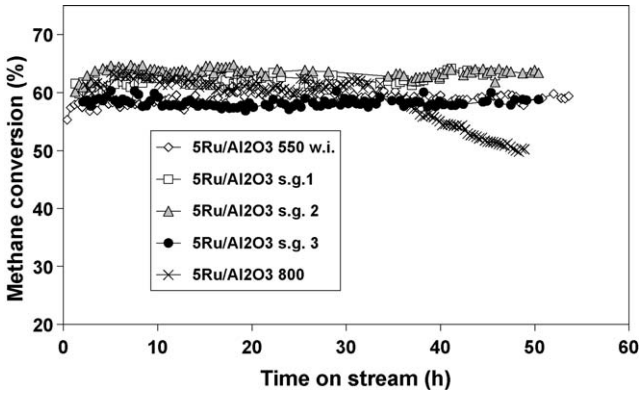

Fig. 6. Methane conversion during LTCPO for the ruthenium catalysts.

169.1 eV [16], and it seems that this SO_4^{2-} species could be adsorbed on the ruthenium particles and on the Al_2O_3 support [16].

3.2. Activity tests

3.2.1. LTCPO free of sulphur

The performance of the rhodium and ruthenium catalysts in the LTCPO of methane at 550 °C was very similar regarding catalyst stability. Only the 5Ru/Al_2O_3 800 w.i. was deactivated after 30 h on stream (Fig. 6). The most active ruthenium catalysts were the 5Ru/Al_2O_3 s.g. 1 and 5Ru/Al_2O_3 s.g. 2, with a methane conversion of 63% (Fig. 7 and Table 6). The 5Ru/Al_2O_3 s.g. 3 and 5Ru/Al_2O_3 550 w.i. were less active, the methane conversion was 59% for both. At higher methane conversion, higher hydrogen, CO and CO_2 yields were obtained. The rhodium catalysts, independent of the preparation technique, had practically the same methane conversion (57%) and the rest of the activity parameters (Fig. 8 and Table 7). For all catalysts at sulphur-free conditions full conversion of oxygen was observed. Due to the fast and exothermic oxidation reactions, hot spots could not be completely avoided. The hot spot temperatures were similar for the ruthenium and rhodium catalysts (about 60 K, Fig. 9). We therefore conclude that this hot spot temperature did not influence the outlet gas composition significantly. Control experiments without catalysts (blank tests) and with the 5Ce–ZrO_2 and γ-Al_2O_3 (JM) supports only exhibited no activity (Tables 6 and 7). The equilibrium data included in Tables 6 and 7 were calculated with Aspen Plus 12.1 (Aspentech, Cambridge, USA).

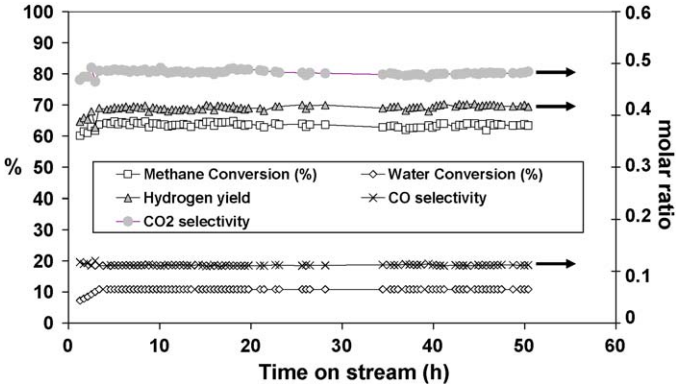

Fig. 7. Activity results for LTCPO of methane for 5Ru/Al_2O_3 s.g. 2 at a WHSV of 65 $g_{feed}\ g_{cat}^{-1}\ h^{-1}$.

3.2.2. LTCPO with 10 ppm of thiophene

Figs. 10 and 11 show the effect of adding 10 ppm of thiophene to the feed on the rhodium and ruthenium catalysts under LTCPO conditions. At this thiophene concentration the Rh catalysts suffered from a very strong deactivation within a few hours on stream. After this initial drop, the catalysts maintained a conversion of over 29% for Rh sol–gel and 34% for w.i. catalysts during the time on stream (Fig. 10 and Table 7). Obviously the hydrogen, CO, and CO_2 yields were also decreased, and the CO_2 selectivity was increased. Total oxygen conversion was observed. Although the ruthenium deactivation was high, the hot spot

Table 6
LTCPO of methane on different Ru catalysts and thiophene concentrations.

Catalyst	Thiophene (ppm)	CH_4 conversion (%)	H_2O conversion (%)	CO_2 selectivity (%)	O_2 conversion (%)	H_2 yield	CO yield	CO_2 yield
Equilibrium	10	76.2	17.7	75.0	100.0	0.62	0.18	0.57
Blank	0	0.8	0	100.0	1.3	0	0	0.01
γ-Al_2O_3 (JM)	10	1.2	0	100.0	1.8	0	0	0.08
5Ru/Al_2O_3 550 w.i.	0	59.4	9.3	82.8	100.0	0.39	0.10	0.48
	10	51.5	−4.0	78.0	100.0	0.26	0.11	0.39
	400	2.6	−16.7	100.0	2.1	0	0	0.04
5Ru/Al_2O_3 800 w.i.	0	50.1	−1.3	86.3	100.0	0.28	0.07	0.44
	10	1.1	−17.2	100.0	1.8	0	0	0.02
	400	7.4	−12.7	100.0	2.9	0	0	0.08
5Ru/Al_2O_3 s.g. 1	0	63.0	10.0	81.4	100.0	0.42	0.11	0.48
	10	52.6	0.5	77.2	100.0	0.29	0.13	0.44
	400	8.2	−9.5	100.0	20.4	0	0	0.11
5Ru/Al_2O_3 s.g. 2	0	63.4	10.8	82.3	100.0	0.42	0.11	0.50
	10	60.3	6.0	82.7	100.0	0.39	0.10	0.48
	400	17.1	−9.0	90.0	100.0	0.05	0.02	0.18
5Ru/Al_2O_3 s.g. 3	0	58.6	8.5	82.7	100.0	0.35	0.10	0.49
	10	48.3	−4.0	77.7	100.0	0.24	0.10	0.35
	400	5.1	−10.0	100.0	11.6	0	0	0.05

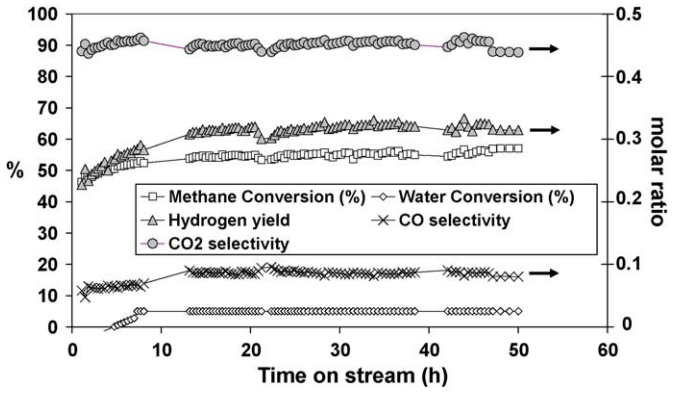

Fig. 8. Activity results for LTCPO of methane for 1Rh/5Ce–ZrO_2 w.i. at a WHSV of 65 $g_{feed}\ g_{cat}^{-1}\ h^{-1}$.

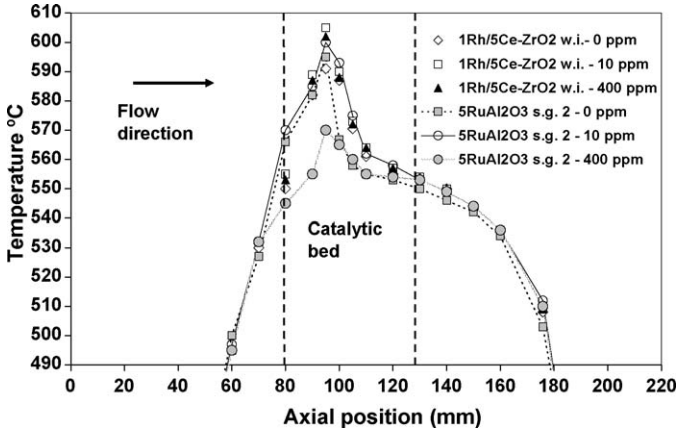

Fig. 9. Gas temperature profiles along the catalytic bed for different levels of sulphur in the feed.

temperature was only slightly higher than for the same catalyst at sulphur-free conditions (Fig. 9). These rhodium catalysts exhibited a certain sulphur tolerance. For the ruthenium catalysts the deactivation was low, with the exception of the 5Ru/Al_2O_3 w.i. 800 catalyst. All the Ru catalysts revealed a slight deactivation. The catalyst which exhibited the highest sulphur resistance was 5Ru/Al_2O_3 s.g. 2 (Fig. 11). For this catalyst the methane conversion decreased only by 3% after more than 50 h on stream compared to the activity under sulphur-free conditions (Table 6). The hydrogen yield was also slightly lower, as were the CO and CO_2 yields, and the CO_2 selectivity was increased slightly. The other ruthenium catalysts revealed a slightly lower sulphur tolerance. In contrast, the sample 5Ru/Al_2O_3 800 w.i. was completely deactivated by 10 ppm of thiophene in the feed. For this catalyst no defined hot spot temperature was observed and the oxygen conversion was only 1.8%, while for the other ruthenium catalysts the oxygen conversion was total and the hot spot temperature was higher than at sulphur-free conditions (Fig. 9).

3.2.3. LTCPO with 400 ppm of thiophene

At this higher concentration of thiophene, the ruthenium catalysts deactivated completely (Table 6). Within 30 h all of these catalysts lost the sulphur resistance that was observed at a level of 10 ppm of thiophene (Table 6 and Fig. 11). No hydrogen was generated, and only a small amount of CO_2 was produced. The oxygen conversion was not complete (with the exception of 5Ru/Al_2O_3 s.g. 2). The hot spot temperature was lower than for the previous conditions. For the rhodium catalysts the behaviour was very similar to the one at 10 ppm (Fig. 10 and Table 7). However, the methane conversion, the hydrogen, CO, and CO_2 yields decreased slightly with respect to the 10 ppm thiophene test, and mainly complete oxidation to CO_2 and H_2O was observed. The CO_2 selectivity was higher than 97%. Also, the oxygen conversion

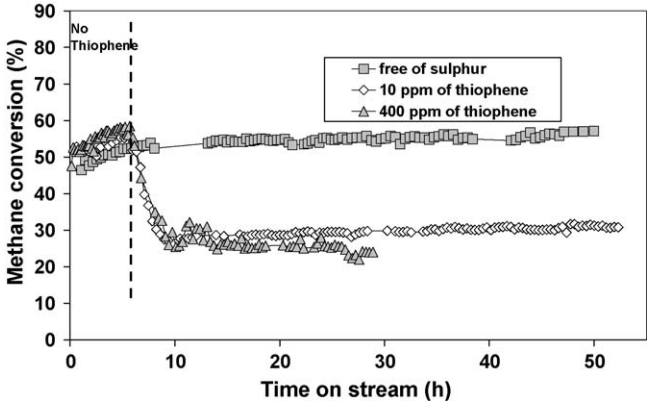

Fig. 10. Activity tests for the LTCPO of methane at different concentrations of thiophene for 1Rh/5Ce–ZrO_2.

was total and the hot spot temperature was higher than for sulphur-free conditions and for 10 ppm of thiophene in the feed.

4. Discussion

For the rhodium catalysts, metallic rhodium is the active phase in LTCPO, and to obtain metallic rhodium, it was necessary to reduce the catalysts. The metal dispersion depends on the technique of preparation. For the sol–gel preparation, a high dispersion was observed by TGA and XPS. However, this higher dispersion had no influence on the catalytic activity. Both catalysts showed the same activity for the LTCPO free of sulphur, and for the LTCPO with 10 and 400 ppm of thiophene. For the LTCPO free of sulphur, the methane conversion and the other activity parameters

Table 7
LTCPO of methane on different Rh catalysts and thiophene concentrations.

Catalyst	Thiophene (ppm)	CH_4 conversion (%)	H_2O conversion (%)	CO_2 selectivity (%)	O_2 conversion (%)	H_2 yield	CO yield	CO_2 yield
Equilibrium	10	76.2	17.7	75.0	100.0	0.62	0.18	0.57
5Ce–ZrO_2	10	0.2	0	100.0	0.8	0	0	0.01
1Rh/5Ce–ZrO_2 w.i.	0	57.1	8.4	84.6	100.0	0.31	0.08	0.44
	10	33.9	−7.9	97.1	100.0	0.09	0.01	0.33
	400	27.2	−9.0	98.4	100.0	0.06	0.01	0.31
1Rh/5Ce–ZrO_2 s.g.	0	57.5	9.2	83.6	100.0	0.34	0.09	0.47
	10	28.9	−8.2	95.7	100.0	0.07	0.01	0.31
	400	22.8	−9.0	97.9	100.0	0.04	0.01	0.23

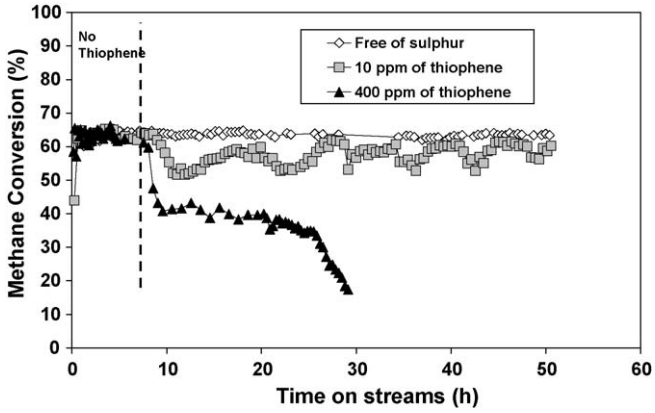

Fig. 11. Activity tests for the LTCPO of methane at different concentrations of thiophene for $5Ru/Al_2O_3$ s.g. 2.

were practically the same for the sol–gel and the impregnation catalysts. No deactivation phenomenon was observed, indicating that the dispersion was maintained during the reaction. In the presence of thiophene, the dispersion was also maintained, as shown by XPS, but the activity decreased. Typically, the deactivation of a noble metal is attributed to the coverage of the metal surface with adsorbed sulphur [3,4]. Recently, Karlajainen et al. [17] showed by thermodynamic calculations that ceria has the tendency to form $Ce(SO_2)_3$ and Ce_2O_2S species in a reducing atmosphere. This behaviour was also obtained in the presence of noble metals. This could explain the observed sulphur tolerance. However, no sulphur could be detected on the catalysts by XPS, neither in the 2p orbital nor in Ce $3d_{5/2}$, or Rh 3d. With XPS the presence of Rh_2O_3 was detected, but Rh_2O_3 shows a low activity for syngas production, as total oxidation products are mainly formed [18]. This was confirmed by the results obtained in the activity tests. The presence of thiophene modified the product distribution: at the higher thiophene concentration more total oxidation products were formed (higher CO_2 selectivity and H_2O yield, and on the other hand lower CO and H_2 yields, Table 6). These results are in agreement with the findings of Bitsch-Larsen et al. [19] and Ferrandon et al. [20]. They have attributed this change in yield and selectivity to the partial oxidation reaction going to complete oxidation and also to the inhibition of the steam reforming reaction. Bitsch-Larsen argued that the absence of a highly endothermic reaction would explain the temperature increase even though the methane conversion drops. This effect was also observed with the rhodium catalysts during the sulphur tests (Fig. 9). Therefore, the presence of thiophene favours rhodium oxidation and the poisoning of the active sites for steam reforming, changing the product distribution. This effect might be due to the limitation of the surface diffusion of H(s) and/or O(s).

The most active ruthenium catalysts at sulphur-free conditions were $5Ru/Al_2O_3$ s.g. 1 and $5Ru/Al_2O_3$ s.g. 2. These catalysts had the highest dispersion (Table 2). All of the ruthenium catalysts were very stable (except $5Ru/Al_2O_3$ 800 w.i.). Nevertheless, sintering occurred during the reaction. The average particle size increased for all the catalysts after reaction (Table 3). The least sintering was observed for the two most active catalysts. The sample $5Ru/Al_2O_3$ s.g. 3 deactivated faster (Table 3, XRD). The ruthenium catalyst calcinated at the higher temperature revealed an unexpected behaviour. For this catalyst no sintering effects were expected due to the calcination temperature of 800 °C and the reaction temperature of 550 °C. But it was the only catalyst that suffered deactivation in the absence of sulphur. After 30 h this catalyst started to deactivate, after showing a high conversion and a stable performance. This behaviour is typical of deactivation by coke formation. Therefore, the high calcination temperature may have affected the electronic structure to favour coke formation. In the LTCPO sulphur test the behaviour depended on the thiophene concentration. At low concentration (10 ppm) the catalysts had a high sulphur resistance (except the $5Ru/Al_2O_3$ 800 w.i.). The ruthenium catalysts revealed a remarkably high resistance against sulphur poisoning. The best one was $5Ru/Al_2O_3$ s.g. 2, which showed only a small deactivation after more than 50 h on stream, compared to the LTCPO at sulphur-free conditions. It seems that the number of active sites is slightly modified in the presence of low concentrations of thiophene (10 ppm). This may be due to a low deposition rate of sulphur compounds at this thiophene concentration. At the higher concentration (400 ppm) sulphur was detected on the catalyst's surface by XPS. This sulphur may be adsorbed on the ruthenium particles and poison the active metal. Hence, this deactivation was attributed to the coverage of the metal surface area with adsorbed sulphur [3,4]. Some evidence for this explanation is the lower oxygen conversion observed at 400 ppm of thiophene with the Ru/Al_2O_3 catalysts (with the exception of $5Ru/Al_2O_3$ s.g. 2), indicating that the active site for partial oxidation is poisoned, probably due to the sulphur adsorption. In addition, the metal dispersion was decreased after reaction (XPS, Table 5). Hence, this lower dispersion and the sulphur adsorption reduced the activity of the ruthenium catalysts.

5. Conclusions

Ruthenium catalysts prepared by a sol–gel method were found to exhibit a promising sulphur resistance at a low thiophene concentration (10 ppm), and among these, the $5Ru/Al_2O_3$ s.g. 2 had the lowest deactivation compared to the LTCPO at sulphur-free conditions. Hence, ruthenium catalysts revealed a remarkably high resistance against sulphur poisoning at a low sulphur concentration.

The presence of a small amount of sulphur has a negative impact on the LTCPO on $1Rh/5Ce–ZrO_2$ sol–gel and wetness impregnation. This is a consequence of the oxidation of the active metal, and probably the inhibition of the steam reforming reaction. Only totally oxidized products were observed with these catalysts. They may still be useful for the catalytic combustion in the presence of sulphur.

Acknowledgements

Assistance and help by A. Frei, M. Schubert, I. Czekai, M. Brandenberger, E. De Boni, A. Rouff, J. Schell, S. Abolhassani-Dadras, and S. Stucki is gratefully acknowledged. This work was financially supported by the Energy Research Programme of the Spanish Ministry for Science and Innovation and by the Basque Autonomous Government (ETORTEK programme).

References

[1] A. Qi, S. Wang, C. Ni, D. Wu, Int. J. Hydrogen Energy 32 (2007) 981.
[2] S. Rabe, T.-B. Truong, F. Vogel, Appl. Catal. A: Gen. 292 (2005) 177.
[3] U. Hennings, R. Reimert, Appl. Catal. B: Environ. 70 (2007) 498.
[4] C. Bartholomew, Appl. Catal. A: Gen. 212 (2001) 17.
[5] M. Ferrandon, T. Krause, Appl. Catal. A: Gen. 311 (2006) 135.
[6] J. Rostrup-Nielsen, J. Sehested, J.K. Nørskov, Adv. Catal. 47 (2002) 65.
[7] J. Rostrup-Nielsen, J.B. Hansen, J. Catal. 144 (1993) 38.
[8] T. Mizuno, T. Nakajima, J. Chem. Eng. Jpn. 35 (5) (2002) 485.
[9] A. Miyazaki, I. Balint, K. Aika, Y. Nakano, J. Catal. 204 (2001) 364.
[10] J. Schulz, A. Roucoux, H. Patin, Chem. Eur. J. 6 (2000) 618.
[11] L. De Rogatis, T. Montini, M.F. Casula, P. Fornasiero, J. Alloys Compd. 451 (2008) 516.
[12] S. Rabe, M. Nachtegaal, F. Vogel, Phys. Chem. Chem. Phys. 9 (2007) 1461–1468.

[13] S. Eriksson, S. Rojas, M. Boutonnet, J.L.G. Fierro, Appl. Catal. A: Gen. 326 (2007) 8.
[14] S. Eriksson, M. Wolf, A. Schneider, J. Mantzaras, F. Raimondi, M. Boutonnet, S. Järas, Catal. Today 117 (2006) 447.
[15] S. Rabe, T.-B. Truong, F. Vogel, Appl. Catal. A: Gen. 318 (2007) 54–62.
[16] H. Wakita, Y. Kani, K. Ukai, T. Tomizawa, T. Takeguchi, W. Ueda, Appl. Catal. A: Gen. 283 (2005) 53–61.
[17] H. Karlajainen, U. Lassi, K.R. Tolonen, V. Kroger, R. Keiski, Catal. Today 100 (2005) 291.
[18] K. Heitnes Hofstad, J.H.B.J. Hoebink, A. Holmen, G.B. Marin, Catal. Today 40 (1998) 157.
[19] A. Bitsch-Larsen, N.J. Degenstein, L.D. Schmidt, Appl. Catal. B: Environ. 78 (2008) 364.
[20] M. Ferrandon, J. Mawdsley, T. Krause, Appl. Catal. A: Gen. 342 (2008) 69.